Influence of the Glass Transition Temperature Gradient on the Nonlinear Viscoelastic Behavior in Reinforced Elastomers

H. Montes,* F. Lequeux, and J. Berriot

ESPCI, 10 Rue Vauquelin, 75005 Paris, France

Received April 10, 2003; Revised Manuscript Received June 24, 2003

ABSTRACT: We analyze the influence of a glass transition gradient near the particle surfaces on the nonlinear mechanical behavior of reinforced elastomers. We studied systems consisting of grafted silica particles dispersed in a cross-linked poly(ethyl acrylate) matrix. Both particle/matrix interfaces and dispersion states of the particles have been precisely characterized. On the basis of previous studies on the same systems evidencing a glass transition gradient around the particles, we show that the precocious nonlinear mechanical behavior of these filled systems is related to the strain-softening of the glassy polymer shell surrounding the particles surfaces. Comparing strain-softening and melting of the glassy polymer shell, we observe that the strain-softening is enhanced by strong local stress amplifications.

Introduction

Filled rubber, consisting of solid particles—either carbon black or silica—dispersed in an elastic matrix, has been widely used for more than 50 years. The role of the solid particles is to reinforce the elastic matrix, increasing elastic modulus, fracture, and abrasion properties. However, most of their mechanical properties are far from being understood. This is mostly due to the intricate effects of solid particles arrangements in the elastic matrix and of modifications of the polymer dynamics near the surface of the particles. These two effects have been the objects of various approaches.

First, the arrangement of the particles—generally dispersed as fractal aggregates—contributes in a complex manner to both the linear and the nonlinear mechanical properties of filled rubbers, and various approaches have been proposed in the past and more recently.[1−4] The main idea is that fractal aggregates can strongly increase the elastic modulus. But under strain there is an evolution of their fractal geometry leading to a decrease of the value of the elastic modulus. This so-called hydrodynamic reinforcement effect is however difficult to quantitatively describe, as it requires a very precise knowledge of the particles' arrangement.

Second, the modification of the polymer dynamics near the surface of the particles has been more puzzling. It has been suggested that dynamics of adsorption/desorption of the polymers chains at the particle surface may be responsible for various linear and nonlinear effects.[5,6] Here, we present results on samples where the polymer chains are strongly anchored, through covalent bonds to the surface of the particles. Thus, the effects of polymer adsorption−desorption are not relevant in our case. Otherwise, in the past, it has been suggested by Struik and others authors[7−10] that the particle/elastomer interface generates around each particle a shell of glassy polymer. For instance, Struik[7,8] has quenched filled rubber above its glass transition temperature, and he observed a physical aging behavior similar to the one shown by a glassy polymer below its glass transition temperature (T_g). NMR measurements have confirmed the glassy nature of the polymer chains near the particles surface.[9,10] This idea was recently improved in introducing the concept that there is a gradient of glass transition temperature around each particle. This was first suggested in ref 11 and quantified by us, on model filled elastomers, using both NMR and mechanical data.[12,13] This idea is also confirmed by the various experiments of T_g measurements performed on polymer films casted on various substrates.[14−17] Last, this is consistent with recent simulations,[18,19] and some theoretical explanations were proposed recently.[20] Actually, we will show in this paper that this concept can also help to understand mechanical nonlinearities in filled elastomers.

In fact, as explained in ref 3, the combination of the two effects—surface dynamics of polymers and particles' arrangement in the sample—is required to explain the mechanical properties of filled rubber. But the building of a theoretical frame combining these two effects is difficult and is still a challenge for the community.

In this paper we will focus on the role of the polymer dynamics near the particle surface on the nonlinearity shown by the dynamical elastic modulus for small values of strain, typically below 100%. This nonlinearity is in fact a decrease of the dynamical elastic modulus for increasing the strain amplitude and has been known for years as the Payne effect in the reinforced elastomer community.[21] In this paper we will show how the gradient of glass transition is responsible for the Payne effect in filled rubbers.

The paper is organized as follows. First, we recall the sample preparation procedures and present the mechanical measurements. Then we recall how we have evidenced the gradient of glass transition on filled elastomers, using linear mechanical properties. Then we discuss the Payne effect in the frame of this concept. According to bulk polymers behavior, we assume that the glassy polymer chains near the particles soften under strain. We then validate this assumption using an original time−temperature superposition for the nonlinear dynamical elastic modulus. Finally, we discuss the possibility of comparing temperature vs stress effects for the nonlinearities of the dynamical modulus. We suggest last a hand-waving description of the stress heterogeneities that provides a qualitative description of the observed effects.

* Corresponding author. E-mail Helene.montes@espci.fr.

10.1021/ma0344590 CCC: $25.00
Published on Web 09/16/2003

Table 1. Characteristics of the Reinforced Sample Sets and the Nonreinforced Elastomer Matrix

set name	mean silica diam (nm)[a]	grafting density Γ (nm^{-2})	e_{graft} (nm)	cross-linker concn[b] (%)	$\langle f_{Si}^N \rangle$ (nm^{-2})[c]	ν_{tot}/ν_e[c]	δ (nm)[c]
EA				0.3		1.58	
MCS_I/C*	45 ± 5	1.6 ± 0.5	0.52	0.3	2.25	[1.84, 3][d]	0.12
ACS/C**	54 ± 7	2. ± 0.5	0.3	0.3	0	1.58	<0.1
MCS_II/H***	50 ± 7	2.8 ± 0.5	0.6	0.3	1.0	[1.67, 1.9][d]	0.25
TPM_III/C*	80 ± 7	10.5 ± 1	1.3	0.3	1.7	[1.7, 2][d]	0.5
TPM_VI/C*	50 ± 7	1.5 ± 0.5	0.3	0.3	1.1	[1.6, 2]	0.2

[a] From SANS measurements.[21] Dispersion state from SANS measurements: *, there is an exclusion radius around the particles; **, presence of large aggregates; ***, there is the coexistence of any linear aggregates with single particles. [b] Per mole of ethyl acrylate monomers. [c] From ^{1}H NMR measurements.[23] [d] Depending on the silica volume fraction.

Experimental Section

A. Sample Preparations. The mechanical measurements were performed on cross-linked poly(ethyl acrylate) chains reinforced with grafted silica particles. The process used for their synthesis has been presented in detail in a previous paper.[22] We briefly recall here the main steps of the preparation.

Following the process developed by Ford and Mauger,[23,24] spherical silica particles are prepared using the Stöber method. They are either transferred to propyl carbonate before to be grafted by monochlorosilane molecules—3-(methacryloxy)propyldimethylchlorosilane (MCS) or acetoxyethyldimethylchlorosilane (ACS)—or directly grafted in the Stöber solution with 3-(trimethoxysilyl)propyl methacrylate (TPM). The grafted silica are then transferred by successive dialysis to methanol and then to ethyl acrylate monomers. From a concentrated parent suspension of silica particle in acrylate monomers, many solutions with various silica concentrations are prepared by dilution with acrylate. A photosensitive initiator (Irgacure from Ciba) and a cross-linker (butanedioldiacrylate) are then added to each dispersion. The polymerization and the cross-linking reaction occur simultaneously by UV illumination.

Note that for every system the cross-linker concentration was kept equal to 0.3% per mole of acrylate monomers. The grafting density Γ was measured by elemental analysis, and we have deduced the thickness of the layer e_{graft} composed of the grafters. The shape and the size of the particles were characterized by small-angle neutron scattering (SANS).[22] These measurements have also shown that the particle surfaces were smooth.

B. Sample Characterizations. The four sample sets studied in this work have been characterized by many ways.[22,25,26] We have summarized in this section the main results. We have taken the nomenclature used in ref 22.

The first and the second sets referred to as MCS_I and MCS_II consist of cross-linked ethyl acrylate chains reinforced with silica particles grafted with the 3-(methacryloxy)propyldimethylchlorosilane (MCS). The samples belonging to the third set contain silica particles grafted with acetoxyethyldimethylchlorosilane (ACS) and are referred to as ACS. The fourth and fifth sets referred to as TPM_III and TPM_VI contain silica particles grafted with the 3-(trimethoxysilyl)propyl methacrylate (TPM). The particles have a diameter around 50 nm, except for the TPM_III samples where the particle size is 80 nm.

The MCS and ACS grafters molecules have only one group able to react with the hydroxyl groups located at the particle surface. ^{29}Si NMR measurements have shown that the MCS and the ACS grafters form brushes over the particle surface. At the opposite, the TPM molecules have three methoxy groups and form a dense and highly cross-linked shell around the particle surface.

Moreover, the MCS and the TPM molecules have a methacrylate group and can then copolymerize with the acrylate monomers during the polymerization step. At the opposite, the ACS grafters cannot form covalent bond with the monomers. The existence of a covalent bond between the MCS- or TPM-coated particles and the elastomer matrix have been confirmed by both swelling measurements[26] and ^{1}H NMR spectroscopy which was used to measured the total topological constraints density ν_{tot} of each sample.[25] The average functionality $\langle f_{Si} \rangle$ of the particles has been deduced from the ^{1}H NMR measurements. The same analysis has confirmed that the ACS particles are not connected to the elastomer matrix.

All these measurements lead to the conclusion that the particles and the elastomer matrix are covalently bonded for the MCS_I, MCS_II, TPM_III, and TPM_VI sets. On the contrary, the particles are not covalently connected to the polymer chains in the ACS reinforced samples.

The arrangement of the particles in the polymer matrix has also been characterized by SANS. The MCS_I, TPM_III, and TPM_VI samples have a very good dispersion state; i.e., the particles seem to have an exclusion shell around them and behave as repelling one another. On the contrary, we observed the presence of a few linear aggregates coexisting with single particles in the MCS_II samples while the ACS elastomers contain large fractal aggregates. These three types of dispersion will be respectively called very good, bad, and very bad dispersion states in the following. All the structural features of the four sample sets are summarized in Table 1.

C. Mechanical Measurements. The mechanical measurements were performed on a Rheometrics RDA II in simple shear strain with a plate—plate geometry. Samples were disks of 8 mm diameter and 2 mm thickness. They were glued with a cyanoacrylate glue (loctite) on the plates of the rheometer. Mechanical measurements were performed on a temperature range from 303 to 383 K and frequencies between 0.01 and 10 Hz. The data in the nonlinear regime were measured with a deformation mode. The sample was submitted to 10 deformation cycles prior the beginning of each dynamical modulus measurement. Some of the data—linear regime for sets ACS—have already been published in ref 13. For the sake of comparison, the viscoelastic modulus of the matrix—cross-linked poly(ethyl acrylate)—was also performed (see ref 13). The glass transition temperature at 1 Hz was found equal to 253 K. We present now the raw data measured in the nonlinear regime.

Experimental Results

In Figure 1, we have plotted the real part of the dynamical modulus variation with the strain amplitude for various samples, frequencies, and temperatures. It allows to see the effect of temperature, frequency, and dispersion state on the nonlinear mechanical behavior of our systems.

We can first observe that the nonlinear behavior of our filled samples—for the same frequency and temperature—is sensitive to the quality of the dispersion state (compare open circles in Figure 1a,b or see data in Figure 2). For samples with "very good" dispersion—MCS_I, TPM_III, and TPM_VI—in which the particles are surrounded by an exclusion radius, the value of the dynamical modulus remains constant for deformation up to 1 (see Figure 2). But for samples having bad dispersion state, we measure a nonlinear viscoelastic behavior on the same deformation range (Figure 1a,b). The real part of the shear modulus decreases for increasing deformation amplitude while the dissipative

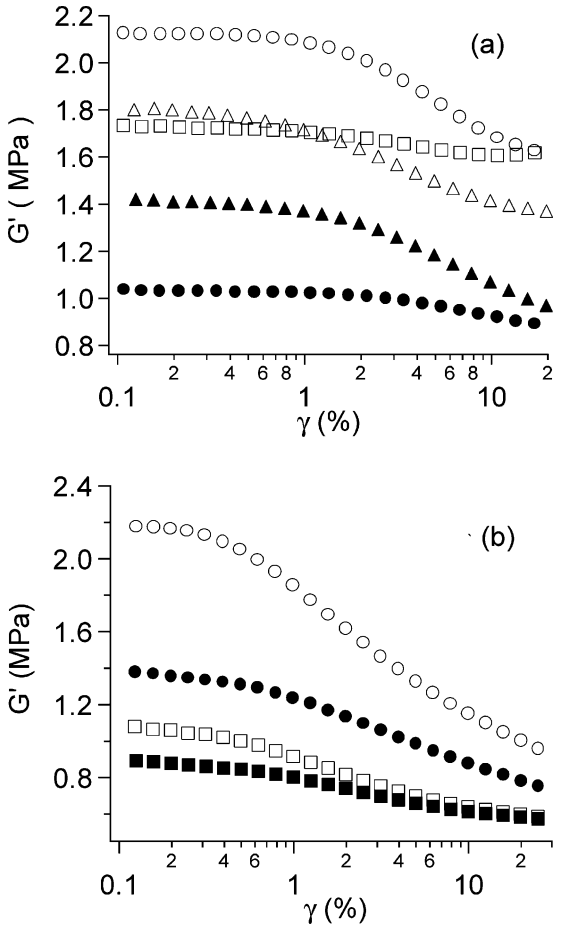

Figure 1. Variation of the real part of the shear modulus G' vs the deformation γ. (a) MCS_II samples $\Phi = 0.21$: (open circle) $\omega = 0.1$ Hz and $T = 303$ K, (open square) $\omega = 0.1$ Hz and $T = 343$ K, (open triangle) $\omega = 0.01$ Hz and $T = 303$ K. $\Phi = 0.15$: (filled circle) $\omega = 0.1$ Hz and $T = 303$ K, (filled triangle) $\omega = 10$ Hz and $T = 303$ K. (b) ACS samples $\Phi = 0.18$: (open circle) $\omega = 0.1$ Hz and $T = 303$ K, (open square) $\omega = 0.1$ Hz and $T = 343$ K, $\Phi = 0.15$: (filled circle) $\omega = 0.1$ Hz and $T = 303$ K, (filled square) $\omega = 0.1$ Hz and $T = 343$ K.

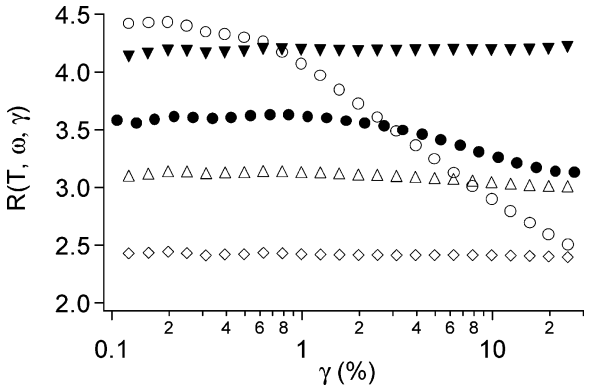

Figure 2. Variation of the reinforcement $R(T,\omega,\gamma)$ of MCS_I, TPM_VI, and TPM_III samples vs deformation at $T = 303$ K: (reversed filled triangle): MCS_I with $\Phi = 0.24$; (open diamond) TPM_III with $\Phi = 0.18$; (open triangle) TPM_VI with $\Phi = 0.18$; (filled circle) MCS_II with $\Phi = 0.15$, (open circle) ACS with $\Phi = 0.15$.

part of the modulus goes through a maximum (data not shown). The modulus variation is larger for the very badly dispersed ACS samples than for the MCS_II samples.

Moreover, the amplitude of the modulus decrease depends on temperature, on frequency, and on silica concentrations. For ACS and MSC_II sample sets, we observed the same main features. The amplitude of the dynamical elastic modulus decrease is larger as the silica concentration increases (compare open and filled circles in Figure 1a,b). In addition, it is lower at higher temperatures (compare circles and squares in Figure 1a,b) or lower frequencies (compare open circles and triangles in Figure 1a). All these effects are sharper for the ACS samples than for the MCS_II samples.

All these features have been observed on many kinds of filled elastomers undergoing an increasing dynamical deformation and is called the Payne effect. The nonlinear behavior shown by our samples is consistent with those observed on other filled elastomers.[11]

How can these nonlinear behaviors be explained? The differences observed between the very well dispersed (MCS_I, MP_III, or TPM_VI) and the very bad dispersed (ACS) samples indicate that the arrangement of the particles strongly influences this nonlinear behavior. However, the temperature and frequency dependence of the Payne effect shows that it does not result in purely geometrical or hydrodynamical effects. Hence, any interpretation must deal not only with the effects of the particle arrangements but also with another temperature- and frequency-dependent mechanism. Moreover, we observed a Payne effect with the MCS_II samples for which the grafted silica particles are covalently bonded to the cross-linked poly(ethyl acrylate) chains. An absorption/desorption picture is thus not appropriate to explain the nonlinearity observed in these filled systems.

On the other hand, it is known for years that the introduction of solid particles in an elastomer matrix leads to a slowing down of the dynamics of the polymer chains located near the particle surface. This slow dynamics looks like the one of polymer chains in the glassy state.[7−12] In the following we analyze the nonlinear behavior of our samples in the frame of the existence of a glass transition gradient near the particle surfaces. We first recall how the existence of a glass transition gradient modifies the mechanical properties of the filled elastomers in the linear regime. Then we extend this concept to the nonlinear regime.

Theoretical Section

A. Theoretical Background: Influence of a Glass Transition Gradient on the Mechanical Properties of Filled Elastomers in the Linear Regime. *A-1. Existence of a Glass Transition Gradient near the Particle Surfaces.* New insights for the understanding of the dynamic modification of a molten polymer near a surface have been obtained from experiments on thin polymer films deposited on a solid substrate. Many experiments made on different systems and by different authors[14−17] have revealed that the glass transition temperature of thin polymer films is shifted compared to the one measured in the bulk. For polymer films strongly absorbed on a substrate, it has been observed that a positive shift of the glass transition temperature of the order of 30 K can be observed for polymer films of 10 nm thickness. It has then been suggested that the glass transition of a polymer is shifted because of the presence of the interface. Recently, a theoretical approach has proposed an interpretation of this phenomenon. According to ref 20, there would be a glass transition temperature gradient at the substrate surface. Let us recall briefly this approach.

The existence of a glass transition gradient near a surface is seen as a consequence of the physical origin of the glass transition. The glass transition can be naively viewed as the following: thermodynamical density fluctuations result in dynamical heterogeneities, which are present in any molecular glasses, because the dynamics is extremely sensitive to the density. Thus, this suggests that the glass transition would originate in the percolation of the densest, or slowest, domains. In other words, at the glass transition, the rigidity originates in the existence of a skeleton of slow domains.

As the percolation threshold varies with the sample dimensionality, the glass transition of a thin film, which corresponds to a nearly-2d geometry, should be different to the one of the bulk-3d geometry. Moreover, the percolation threshold depends also on the interactions at the polymer/substrate interface. For polymer films strongly interacting with the substrate, the threshold is lower due to the emergence of additional rigid paths through the substrate. According to ref 20, the glass transition at a given frequency T_g^{ω} would vary with the distance z to the substrate surface following the equation

$$T_g^{\omega}(z) = T_g^{\omega}(1 + (\delta/z)^{\nu}) \quad (1)$$

where δ is the length controlling the amplitude of the gradient and T_g^{ω} is the bulk glass transition at the frequency ω. The exponent ν is equal to 0.88. This law is nearly similar to the one suggested by Keddie[14] and observed on polymer films when the radius of gyration of the chains is smaller than the film thickness.

The existence of such glass transition gradient was intuited by Wang[11] to be at the origin of the modification of the filled elastomers mechanical properties in the linear regime. We have recently shown[13] that this concept allows to describe quantitatively some properties of the linear dynamical elastic modulus that we will recall now.

Note: In the following and for the sake of clarity, we sometimes omit the suffix ω. Moreover, the notation T_g corresponds always to the bulk value of the glass transition, while $T_g(z)$ stands for the glass transition temperature modified by a surface at a distance z.

A-2. Temperature−Frequency Superposition for Filled Elastomers in the Linear Regime. As described in ref 13, the hypothesis of the existence of a gradient of glass transition temperature near the particles allows to describe the frequency−temperature dependence of the linear mechanical properties observed on our filled elastomers for T higher than T_g ($T > T_g + 50$).

Actually, the temperature of the glass transition increases for polymers at decreasing distance from the particle interfaces, following eq 1. Thus, above the bulk glass transition temperature the polymer chains are in the glassy state near the particle surface and the polymer chains are in the rubbery state far from the particles. In fact, the elastic modulus varies weakly with temperature, in the two following domains, $T - T_g(z) < -10$ K and $T - T_g(z) > 30$ K. But it varies at least 3 orders of magnitude for $T - T_g(z)$ between −10 and 30 K. As $T - T_g(z)$ varies strongly with the distance to the interface z, the dynamical elastic modulus varies extremely abruptly from its glassy value to its rubbery value. This allows the following coarse-grained approximation for temperature higher than $T_g + 50$ K. We can consider that the polymer chains for which $T_g(z)$ is higher than T are infinitely rigid while the other ones have an elastic modulus equal to the one of the bulk polymer. Thus, we can define a shell of glassy polymer around the particles which thickness e_g is given by $T_g(e_g) = T$ and is temperature-dependent. The glass transition temperature of the matrix is frequency-dependent, and according to eq 1, the thickness e_g will also vary with frequency. This leads to the following expression for e_g:

$$e_g(T,\omega) = \delta(T_g^{\omega}/(T - T_g^{\omega}))^{1/\nu} \quad (2)$$

Let us remark that this temperature dependence of the glassy thickness has been confirmed by NMR measurements.[12,13] The values of δ have been measured for our samples by ^{1}H NMR and are given in Table 1. According to this coarse-grained approximation, the macroscopic modulus is controlled by two parameters: the thickness of the glassy shell and the arrangement of the particle inside the matrix.

Thus, for a given sample, i.e., a given arrangement of particles, the temperature and frequency dependence of the modulus is controlled by the variation of e_g with T and ω according to eq 2. The modulus of the filled sample $G(T,\omega,\Phi)$ is then only fixed by the reduced variable $(T_g^{\omega}/(T - T_g^{\omega}))$. This is expected for any given sample whatever the arrangement of the particles. For instance, if glassy bridges mechanically connect pairs of particles leading to the formation of solid clusters, the morphology of these solid clusters will only depend on the reduced variable $(T_g^{\omega}/(T - T_g^{\omega}))$.

A-3. Experimental Validation of This Temperature−Frequency Superposition in the Linear Regime. This theoretical prediction has been validated by the mechanical data measured on our filled samples.[13] We have shown that the reinforcement $R(T,\omega,\Phi)$, i.e., the modulus of the filled elastomer $G(T,\omega,\Phi)$ divided by the one of the nonreinforced matrix $G(T,\omega,\Phi=0)$, fulfills this temperature−frequency superposition law. Let us remark that the reinforcement, instead of the bare modulus $G(T,\omega,\Phi)$, is used in the master curves in order to take into account the entropic behavior of the polymer chains far from the particle. By entropic behavior we mean the increase of the elastic modulus proportional to temperature above $T_g + 50$ K.

Figure 3a shows the dependence of the reinforcement vs temperature and frequency for MCS_II samples having varying silica concentration. The data were measured for temperature T such that $T > T_g^{\omega} + 50$ K, i.e., in a temperature range where the nonreinforced matrix has an entropic behavior ($G \propto T$). The mechanical behavior of these filled samples clearly departs from the one of the unfilled elastomer in the same temperature range.

A master curve is obtained for each concentration when plotting the reinforcement vs the reduced variable $T_g^{\omega}/(T - T_g^{\omega})$, in agreement with the theoretical predictions in the linear domain (see Figure 3b).

Similar master curves were obtained with the other systems whatever their structure−dispersions states and interactions at the interface. We have shown in ref 13 that this is also valid for the ACS system that have very bad dispersion and weak interactions at the interface. For very well dispersed MCS_I, TPM_III, or TPM_VI, the temperature dependence of the reinforcement is weak (see Figure 4) but visible for the highest silica concentration. Thus, the concept of glass transition

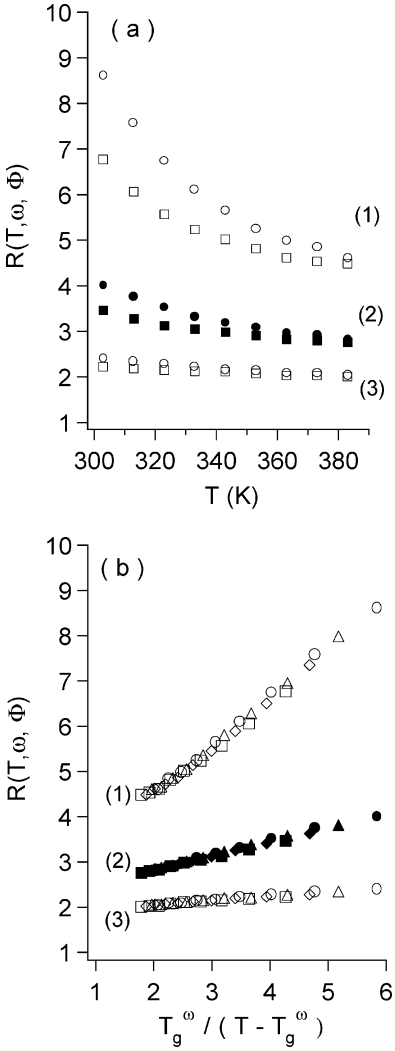

Figure 3. (a) Variation of the reinforcement $R(T,\omega,\Phi)$ with temperature and frequency for MCS_II samples having varying silica concentrations. Measurements were performed in the linear regime. (1) $\Phi = 0.21$, (open circle) $\omega = 10$ Hz, (open square) $\omega = 0.01$ Hz; (2) $\Phi = 0.15$, (filled circle) $\omega = 0.10$ Hz, (filled square) $\omega = 0.01$ Hz; (3) $\Phi = 0.12$, (open circle) $\omega = 10$ Hz, (open square) $\omega = 0.01$ Hz. (b) Shape of the master curves obtained plotting the reinforcement $R(T,\omega,\Phi)$ vs $T_g^{\omega}/(T - T_g^{\omega})$. The labels (1), (2), and (3) correspond to MCS_II samples containing a silica volume fraction Φ of 0.21, 0.15, and 0.12, respectively. The frequency associated with the different data are: in circle $\omega = 10$ Hz, in triangle $\omega = 1$ Hz, in diamond $\omega = 0.1$ Hz, and in square $\omega = 0.01$ Hz.

gradient describes the mechanical behavior observed in the linear regime for the filled elastomers whatever the structure of the sample. Moreover, the absolute values of the reinforcement R is strongly influenced by the dispersion state. The more disordered the arrangement of particles is, i.e., the "worst" the dispersion is, the larger the slope of the reinforcement vs $T_g^{\omega}/(T - T_g^{\omega})$ is.

In conclusion of this part, all our filled systems verify the temperature−frequency superposition law predicted from the existence of a glass transition gradient near the particles surfaces. This result shows that (i) the glassy shell—already revealed by NMR or by physical aging experiments—is in fact induced by the presence of a glass transition temperature gradient near the surface and (ii) the thickness of this glassy layer depends on temperature and frequency. Finally, its impact on the mechanical measurements is enhanced

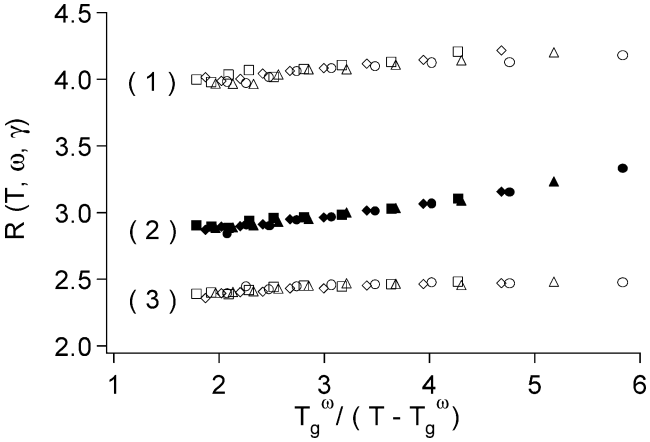

Figure 4. Variation of the reinforcement $R(T,\omega)$ vs $T_g^{\omega}/(T - T_g^{\omega})$ measured on well-dispersed filled elastomers in the linear regime (1) MCS_I with $\Phi = 0.24$; (2) TPM_VI with $\Phi = 0.18$; and (3) TPM_III sample with $\Phi = 0.18$.

by strong particle/matrix interactions, short particle−particle distances, or "bad dispersion" states.

We will now analyze how the existence of a glass transition gradient near the particle surfaces influences the nonlinear behavior of the filled elastomers.

B. Nonlinear Viscoelastic Behavior of Filled Elastomers: Strain-Softening of the Glassy Shells. In this section we will first assume that the glassy shell surrounding the particles surfaces can undergo a strain softening under a large cyclic deformation, similar to what is observed for a bulk polymer. We will then estimate the consequences of this assumption for the nonlinear mechanical properties of filled rubbers. We will then compare our experimental results with our prevision. Let us first recall the main features of the nonlinear behavior of a bulk glassy polymer undergoing a cyclic deformation.

B-1. Nonlinear Behavior of a Bulk Glassy Polymer: Strain-Softening under Cyclic Deformation. Despite the complexity of nonlinear mechanics of solid polymers, we aim to describe it quite naively to estimate its consequences for filled rubber. Therefore, we will limit ourselves here to a very schematic description of solid polymer mechanics. The conventional stress−strain curve of a glassy polymer undergoing an unidirectional loading is composed of three distinct regions.[27] In the first domain, the true stress σ increases nearly linearly with the strain γ up to the yield point characterized by its deformation γ_y and its yield stress σ_y. Beyond the yield point there is a fall in true stress such that the ratio $\sigma/(G_g\gamma)$ decreases as the deformation increases (G_g is the elastic modulus in the glassy state). It varies typically from 1 to 5×10^{-2} for a strain varying from 0% to 50%. This is commonly known as the strain-softening regime and is observed from the yield point up to a deformation referred to as γ_1. Finally, for deformations larger than γ_1, the ratio $\sigma/(G_g\gamma)$ increases again but remains lower than 1 in this last regime.

The values of the yield stress and of the yield deformation are temperature-dependent: both increase for decreasing temperature. Actually at a given loading rate the yield stress σ_y varies linearly with temperature according to the well-known empirical relation[24,27,28,29]

$$\sigma_y \sim K_y(T_g - T) \tag{3}$$

where K_y is of the order 1 MPa K^{-1}.

Moreover, the stress-softening observed beyond the yield point is attributed to the growing up of some rubberlike domains under the loading by many authors. They have shown that a strain-softened glassy polymer is constituted by rubberlike domains embedded in a glassy matrix.[30,31]

What happens now if a cyclic instead of a monotonic deformation is applied to a bulk glassy polymer? Under cyclic deformation, after a few cycles, the mechanical response becomes stable and apparently linear. By *apparently linear* we mean that, under a sinusoidal deformation, the response contains mostly only the frequency ω component of the excitation, while the amplitudes for frequencies $n\omega$, where n is an integer larger than 1, are nearly zero, but simultaneously, the response amplitude is not proportional to the amplitude of the solicitation.

Thus, the glassy polymer is characterized by an apparent modulus G_{ap}. This modulus strongly decreases with the strain amplitude. It decreases from its linear value G_g to values even lower than the ratio σ/γ measured on the unidirectional test—this phenomenon being called cyclic softening.[32,33] Moreover, this phenomenon is both temperature- and frequency-dependent.

This observation is reminiscent of the one made by Chazeau et al.[34] on filled rubbers. These authors have shown that, after several deformation cycles of same amplitude, the response of the filled elastomer becomes stationary and almost purely sinusoidal as observed for glassy polymers undergoing a large cyclic deformation. Thus, the assumption that a part of the glassy shells undergoes a cyclic-softening after a few cycles of a large cyclic deformation is perfectly consistent with the observations made both on filled elastomers and glassy bulk polymer.

But let us precisely now introduce our assumption for the strain-softening of the glassy polymer shell.

B-2. Consequences for Filled Elastomers. Hypothesis for the Strain-Softening in Filled Rubber. First let us claim that, as for monotonic loading, the strain-softening of bulk polymers for cyclic softening test originates in the formation of small domains with a rubberlike modulus.

Here we are dealing with cyclic strain-softening of very thin layers of glassy polymer. It is thus reasonable to assume that nanometric polymer films that are strain-softened behave as the rubberlike domains in bulk polymer during cyclic softening.

We can then deduce how the glassy shells can be partly strain-softened as an increasing cyclic deformation is applied to the filled elastomer. We assume here that the glassy polymer chains located at the distance z from the neighboring particle surface behaves under a cycle of amplitude σ, of frequency ω, at temperature T, and in the stationary regime, with the following characteristics: (i) for $\sigma < \sigma_y$ their apparent modulus G_{ap} is of the order of G_g; (ii) for $\sigma > \sigma_y$ their apparent modulus G_{ap} is of the order of the matrix modulus in its rubber state; (iii) their yield stress σ_y is given by $K_y(T_g^{\omega}(z) - T)$. This last assumption combined with the existence of a glass transition gradient leads to the existence of a gradient of yield stress around the particles. The spatial distribution of the yield stress can be expressed using eqs 1 and 3 as

$$\frac{\sigma_y(z)}{T_g^{\omega}} = K\frac{T - T_g^{\omega}}{T_g^{\omega}}\left(1 - \frac{T_g^{\omega}}{T - T_g^{\omega}}\left(\frac{\delta}{z}\right)^{1/\nu}\right) \qquad (4)$$

We now examine the consequences of these assumptions on the mechanics of filled elastomers.

Consequences for Isolated Particles in a Matrix. In this section, we consider the case of a single particle surrounded by a polymer matrix. This case is representative of filled elastomers such that all the particles are well separated from their neighbors, as in a colloidal crystal, and such that, in the considered temperature range, there are no glassy bridges between particles. This is commonly identified as a sample with "a very good dispersion state".

Now, let us apply a macroscopic stress Σ to the sample. Because of the heterogeneities of the system, the stress is redistributed in a stress field $\sigma(\mathbf{r})$ where $\mathbf{r}$ is the position in the sample. But in the case of isolated particles, one can show that, assuming an incompressible elastomer, the ratio between the local and the macroscopic stress remains between 0 and $^5/_2$.[36] Thus, this stress redistribution is weak in this case. However, the polymer matrix such that $\sigma(\mathbf{r}) = \sigma_y(z(\mathbf{r}))$ undergoes a plastic deformation leading to their strain-softening. Here $z(\mathbf{r})$ is the distance between the point $\mathbf{r}$ and the nearest interface.

Thus, this strain-softening leads to a decrease of the apparent modulus of the polymer chains located at a distance z such that $\sigma_y(z(\mathbf{r})) = \sigma(\mathbf{r})$.

In the case of a single particle, there is thus an about isotropic strain-softening of the glassy layer around the particle. If we assume, like in ref 13, that the modulus of the nonsoftened glassy polymer chains is infinitely rigid—as compared to the polymer in the rubber or strain-softened state, the coarse-grained approximation is then straightforward. In this frame, we can then express the variation of the thickness of the glassy polymer layer e_g with the local stress σ. Moreover, the local stress σ is approximately equal to the macroscopic one Σ as the particles are isolated. We can thus defined the thickness $e_g(\Sigma)$ at temperature T such that the polymer chains located at $z > e_g$ are either in the rubber state or strain-softened. This corresponds to the following:

$$T_g(e_g(\Sigma)) - \Sigma/K_y \approx T \qquad (5)$$

leading to the relation

$$e_g(\Sigma) \approx \delta(T_g^{\omega}/(T - T_g^{\omega} + \Sigma/K_y))^{1/\nu} \qquad (6)$$

Hence, the thickness of the glassy layer decreases for increasing stress amplitudes. However, this equation is valid only if the stress is nearly homogeneous and thus for large distances between particles. But in general the distance between particles is widely distributed, and the local stress can be very different from the macroscopic one.

Real Filled Systems. In a real system, the distance between two particle surfaces is widely distributed, and glassy bridges eventually connect pairs of neighboring particles or even clusters. The existence of glassy bridges between particles leads to a strongly heterogeneous distribution of the stress field within the sample that complicates the response of a real filled system compared to the one with isolated particles. Indeed, the stress distribution in the sample is very sensitive to the

morphology of the rigid inclusions formed by the particles and the glassy bridges connecting them. Hence, if we assume that part of the glassy phase is strain-softened as a large macroscopic deformation is applied, the morphology of the rigid inclusions changes leading to a redistribution of the stress within the sample.

In a Payne experiment, for each deformation amplitude, few deformation cycles are applied before the modulus measurement is performed. It results that the scenario for the macroscopic strain-softening is quite complex. During the first deformation cycle, the polymer chains such that $\sigma(\mathbf{r}) = \sigma_y(z(\mathbf{r}))$ are strain-softened. This partial strain-softening leads to new stress distribution in the sample such that, during the following deformation cycles of the same amplitude, new glassy polymer chains are strain-softened. This progressive strain-softening of a part of the glassy layers continue until a state is reached where all the domains where $\sigma(\mathbf{r}) = \sigma_y(z(\mathbf{r}))$ are strain-softened—$\sigma(\mathbf{r})$ depending itself on the strain-softened domains geometry. The filled elastomer reaches then a stationary response that is "apparently linear", similar to cyclic-softened bulk polymer, as observed by Chazeau et al.[34]

At least for each amplitude variation, a new state of this complex strain-softening arrangement is reached.

To summarize, in the frame of our assumption an increasing macroscopic stress leads to a strain-softening of the glassy polymer shells. Thus, it results in a decrease of the glassy polymer volume and finally of the dynamical elastic modulus, but the response remains purely sinusoidal, i.e., "apparently linear". This allows to explain qualitatively the Payne effects observed in reinforced elastomers. We will see now that despite its complexity the Payne effect may exhibit, in the frame of our assumption, some specific properties. First, we predict a frequency−temperature superposition in the linear regime. Second, we will be able to discuss the respective effects of the stress amplitude and the temperature on the morphology of the glassy shell.

B-3. Master Curves for the Nonlinear Elasticity of Filled Elastomers. Temperature−Frequency Superposition in the Nonlinear Regime. In the nonlinear regime, the morphology of the solid inclusions depends on both the reduced variable $T_g^{\omega}/(T - T_g^{\omega})$ and the spatial distribution of the yield stress given by eq 4. The nonlinear variation of the dynamical modulus only depends on the arrangement of the glassy shell which is determined by the equation $\sigma_y(z(\mathbf{r})) = \sigma(\mathbf{r})$. Because the local yield stress divided by T_g^{ω} is a function of the reduced variable $T_g^{\omega}/(T - T_g^{\omega})$ alone (as shown in eq 4), we can assert the following law: for a given sample and at a given value of $T_g^{\omega}/(T - T_g^{\omega})$, the nonlinear dynamical modulus will depend only on Σ/T_g^{ω} where Σ is the macroscopic stress applied to the sample.

Finally, this means that for a given sample, i.e., a fixed particle dispersion state, the reinforcement $R(T,\omega,\Sigma)$ is only a function of two parameters: Σ/T_g^{ω} and the variable $T_g^{\omega}/(T - T_g^{\omega})$. Let us recall that this new nonlinear law is only valid in the frame of our coarse-grained approximation, i.e., in the approximation of an infinite mechanical contrast between glassy polymer and rubber or strain-softened polymer. This approximation fails if $T < T_g + 50$ K.

In Figure 5a, we have plotted the dynamical modulus, divided by its value at vanishing amplitude, as a function of the stress amplitude divided by T_g^{ω} for a MCS_II sample containing 0.21 (vol) silica particles.

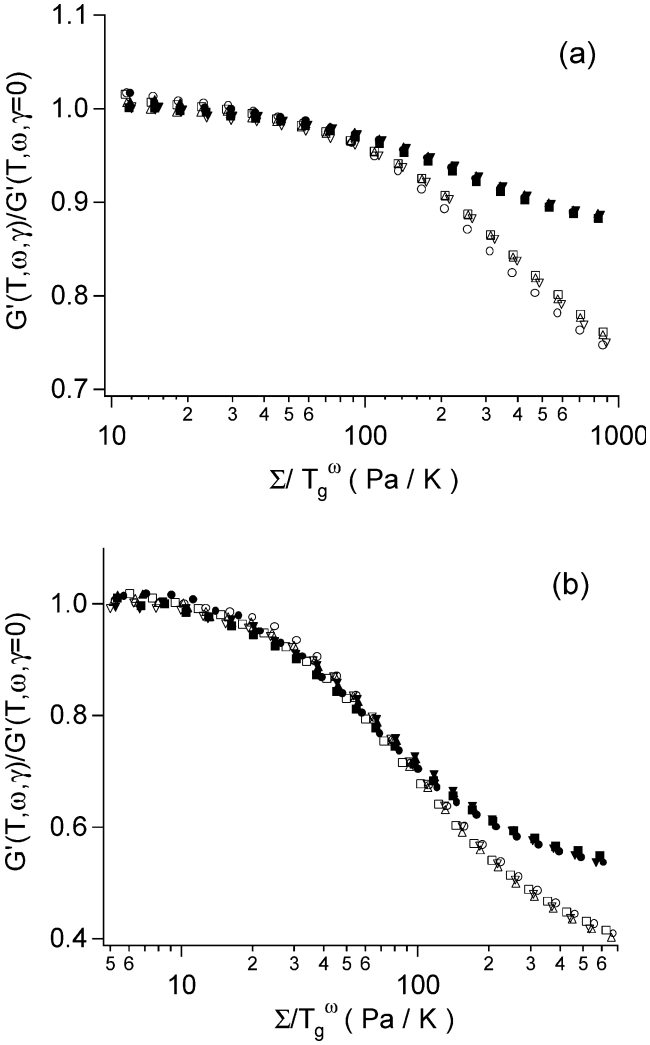

Figure 5. Master curves showing the dependence of the normalized real part of the shear dynamical modulus $G'(T,\omega,\gamma)/G'(T,\omega,\gamma = 0)$ on the deformation γ at constant $T_g^{\omega}/(T - T_g^{\omega})$. (a) MCS_II sample with $\Phi = 0.214$. $T_g^{\omega}/(T - T_g^{\omega}) = 3.783$: (open circle) $\omega = 0.01$ Hz and $T = 308.5$ K, (open square) $\omega = 0.1$ Hz and $T = 314$ K, (open triangle) $\omega = 1$ Hz and $T = 319.5$ K, (reversed open triangle) $\omega = 10$ Hz and $T = 325$ K. $T_g^{\omega}/(T - T_g^{\omega}) = 2.464$: (filled circle) $\omega = 0.01$ Hz and $T = 343$ K, (filled square) $\omega = 0.1$ Hz and $T = 348.5$ K, (filled triangle) $\omega = 1$ Hz and $T = 354$ K, (reversed filled triangle) $\omega = 10$ Hz and $T = 359.5$ K. (b) ACS sample with $\Phi = 0.18$. $T_g^{\omega}/(T - T_g^{\omega}) = 3.783$: (open circle) $\omega = 0.01$ Hz and $T = 308.5$ K, (open square) $\omega = 0.1$ Hz and $T = 314$ K, (open triangle) $\omega = 1$ Hz and $T = 319.5$ K, (reversed open triangle) $\omega = 10$ Hz and $T = 325$ K. $T_g^{\omega}/(T - T_g^{\omega}) = 2.464$: (filled circle) $\omega = 0.01$ Hz and $T = 343$ K, (filled square) $\omega = 0.1$ Hz and $T = 348.5$ K, (filled triangle) $\omega = 1$ Hz and $T = 354$ K, (reversed filled triangle) $\omega = 10$ Hz and $T = 359.5$ K.

This plot has been performed for two values of $T_g^{\omega}/(T - T_g^{\omega})$: 3.783 and 2.464. At a fixed $T_g^{\omega}/(T - T_g^{\omega})$ all the data superimpose on a master curve. But the shape of the master curve changes with the value of $T_g^{\omega}/(T - T_g^{\omega})$. Similar results were obtained with the ACS sample having a silica volume fraction of 0.18 (see Figure 5b).

These results show that the dynamical modulus of a given reinforced sample in the nonlinear regime depends, as expected in the frame of our assumptions, only on the quantities Σ/T_g^{ω} and $T_g^{\omega}/(T - T_g^{\omega})$. It shows that, similar to the value of the linear elastic modulus, the value of the nonlinear modulus in the Payne regime only depends on the glass transition gradient arrangement in the sample. It thus evidences that the decrease of

the modulus observed for increasing deformation amplitude (or stress amplitude) results from the strain-softening of the glassy shell in our systems. It thus confirms the validity of our hypothesis: the Payne effect originates in the strain-softening of the glassy polymer, their glassiness being induced by the existence of a gradient of T_g. In addition, as expected, the shape of $R(\Sigma/T_g^{\omega}, T_g^{\omega}/(T - T_g^{\omega}))$ varies with the dispersion state of the samples. We will discuss this point in the next section.

Discussion

A. Strain-Softening of the Glassy Shell at the Origin of the Payne Effect. We have recently shown that the linear viscoelastic behavior of our filled elastomers is governed by the glass transition gradient near the particle surface combined with the particles arrangement within the elastomer matrix. If an increasing sinusoidal stress is applied to a reinforced system, its dynamic modulus decreases while the modulus of the nonreinforced matrix remains constant. The stress dependence of the modulus depends on both temperature and frequency. We showed in this work that for a given sample this nonlinearity of the dynamic modulus is controlled by the initial thickness of the glassy shell e_g^0 and by the amplitude of the mechanical solicitation. Thus, the strain-softening of the glassy shell surrounding the solid particles is responsible for the Payne effect in our case. Moreover, the amplitude of the Payne effect is governed by the arrangement of the particles in the sample, as discussed now.

In the well-dispersed MCS_I and TPM_III samples we did not succeed to detect any nonlinear viscoelastic behavior for deformation amplitude lower than 1. For these samples the distances between particles surfaces—typically between 10 and 60 nm depending on the silica concentration—are larger than the expected glassy layer thickness, about 3 nm at $T_g + 50$ K. On the opposite, we observe Payne effect with MSC_II and ACS samples that contain aggregates, i.e., in which a part of the distances between particles are lower than e_g. Thus, we observe experimentally that the strain-softening of nonoverlapping glassy shells requires higher macroscopic stress than the strain-softening of glassy bridges. The absence of Payne effect in well-dispersed samples is consistent with our estimations. If we assume that the local stress is about the macroscopic stress, using eq 6, we can estimate that a decrease of the glassy shell from 3 to 2 nm requires a strain amplitude of 10! Thus, the strain-softening process around isolated particles is negligible. Finally, this proves that the nonlinear behavior of $G'(\Sigma)$ is mainly controlled in our filled systems by the strain-softening of the glassy bridges connecting solid particles. We will come back to this point later on.

B. Comparison of Slow Dynamics in Filled Elastomers and Glassy Polymers. The concept of the glassy polymer shell explains also the modulus recovery observed after the application of few cycles of a large deformation on our filled elastomers. After the cessation of the sinusoidal deformation, we observed a logarithmic drift of the linear dynamical elastic modulus: the elastic modulus increases logarithmically until it reaches its initial value measured on the sample in the linear regime. The recovery fraction of the dynamical modulus is about 0.5 at the end of few seconds. However, the whole modulus recovery requires several hours. For instance, the recovery of the Payne effect of an ACS/H sample containing a particle volume fraction of 0.16 that has undergone a deformation amplitude of 0.3 at 0.1 Hz and at $T = T_g + 60$ is about 0.4 at the end of 30 s. The whole recovery requires about 1 h. The recovery time decreases for decreasing final deformation amplitude and increasing temperature. Such recovery behavior is similar to the one observed by Chazeau et al.[34] or Lapra[35] on other filled elastomers.

This logarithmic recovery kinetics agrees with observations made by Struik on cold-drawn polymers.[7] An intense pulse of stress leads to a reactivation of aging in the glassy polymer. Struik concluded that cold-drawing has the same effect as a brief heating above T_g. Furthermore, others authors[37,38] observed that a cold-drawn polymer exhibits very slow recovery of its deformation. These experimental results observed in cold-drawn polymers show that the structure of a glassy polymer equilibrates slowly after the application of a large strain or stress. Thus, the logarithmic drift of the modulus observed in filled elastomers after a large sinusoidal deformation is very similar to the slow recovery observed in glassy polymers. After being strain-softened by a large deformation, the glassy bridges reach their equilibrium very slowly similar to what is observed for bulk glassy polymers. Finally, we suggest here that our filled elastomers exhibit several properties reminiscent of bulk glassy polymer, confirming the major role of the glass transition temperature gradient near the particle surface in mechanical properties of our filled elastomers.

C. Equivalence between Strain Amplitude and Temperature in Filled Elastomers. *C-1. Comparison of Effects of Strain and Temperature.* We have shown that the glass transition gradient is at the origin of the decrease of the modulus both with temperature in the linear regime and with the strain amplitude in the nonlinear regime. In the both cases, the modulus decrease is associated with the decrease of the glassy polymer volume within the sample. However, the effect of the macroscopic deformation should not be identical to the one of temperature because the temperature decreases homogeneously the glassy shell thickness, whether the strain-softening remains localized in the domains where the local stress is the largest. Indeed, the reinforcement dependence with the amplitude of the macroscopic deformation Γ is closely related to the way the glassy domains soften under the local stress. For instance, the shape of $R(\Gamma)$ is different according to whether or not there are glassy bridges within the sample. It results that the strain-softening of a given of domain of glassy polymer should occur at different strain amplitudes whether or not it is located within a glassy bridge. On the contrary, a temperature increase induces an homogeneous decrease of the glassy polymer volume within the sample. Thus, a comparison of the strain and the temperature roles should give a deeper insight into the mechanisms controlling the modulus decrease, particularly in the nonlinear regime.

For that aim, we compare now the dependence of the reinforcement with the stress amplitude—at temperature T_0—and the one with the quantity $K_y(T - T_0)$—in the linear regime. We have plotted on the same graph the variations of the reinforcement as a function of temperature in the linear regime and as a function of stress at the temperature T_0. Figures 6a and 7a show the data measured on a MCS_II sample ($\Phi = 0.20$) and a ACS sample ($\Phi = 0.18$), respectively. The temperature

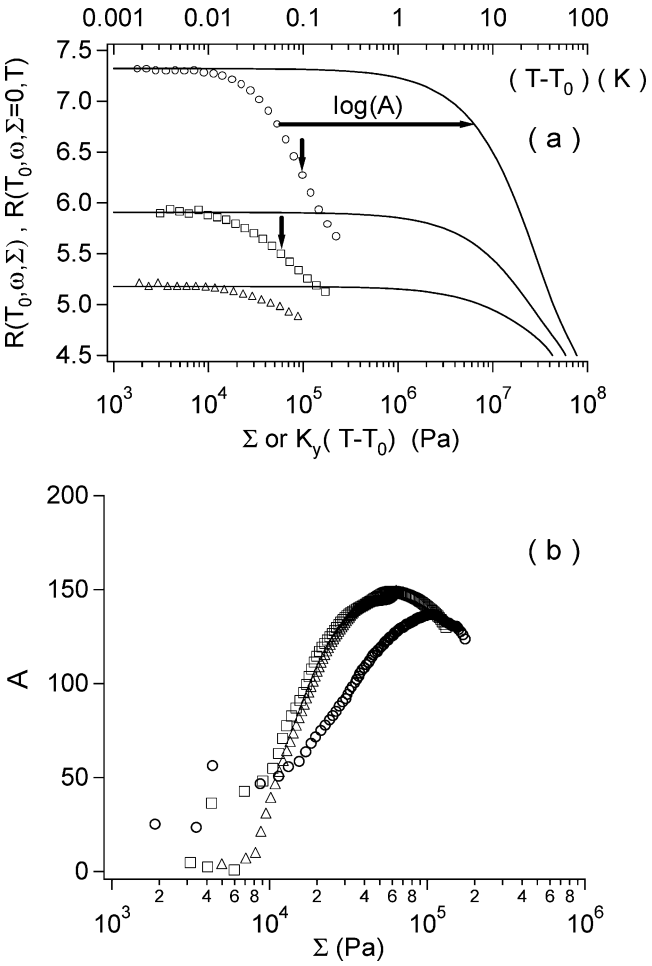

Figure 6. Comparison of the effect of macroscopic stress and temperature on the value of the reinforcement of a MCS_II sample having the silica volume fraction of 0.214. (a) The curves showing the temperature dependence of the reinforcement R_T vs $K(T - T_0)$ are plotted in solid lines ($K_y = 1$ MPa K^{-1}). The variation of the reinforcement with the macroscopic stress Σ are plotted in markers: $T = 303$ K (open circle), $T = 323$ K (open square), and $T = 343$ K (open triangle). (b) Variation of the parameter A with the macroscopic stress Σ for three temperatures: $T = 303$ K (open circle), $T = 323$ K (open square), and $T = 343$ K (open triangle). The arrows in (a) point out the position of the maximum of A observed in (b).

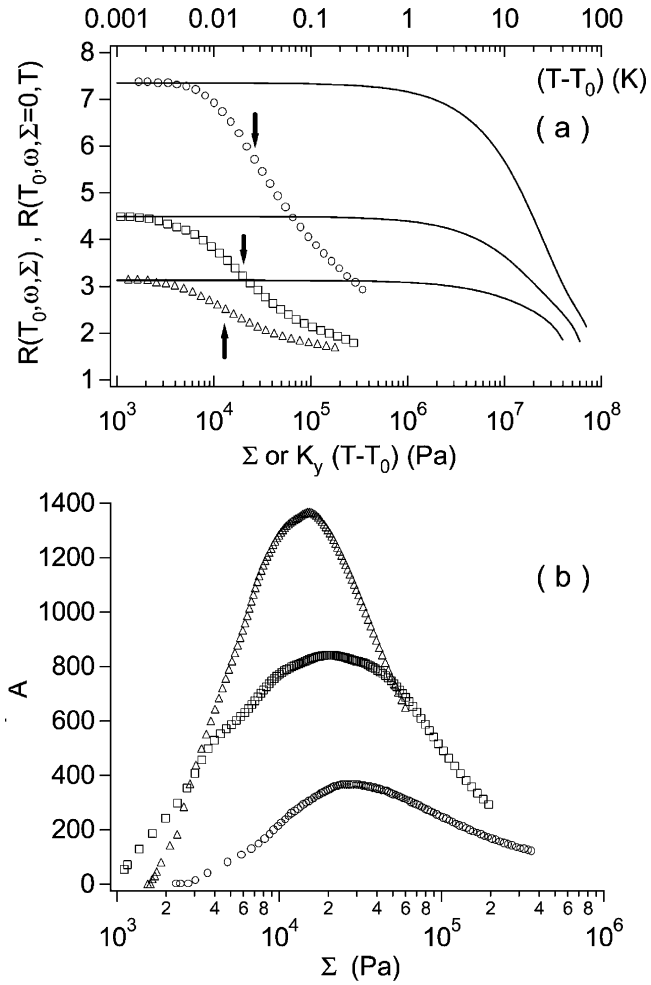

Figure 7. Comparison of the effect of macroscopic stress and temperature on the value of the reinforcement of a ACS sample having the silica volume fraction of 0.18. (a) The curves showing the temperature dependence of the reinforcement R_T vs $K(T - T_0)$ are plotted in solid lines ($K_y = 1$ MPa K^{-1}). The variations of the reinforcement with the macroscopic stress Σ are plotted in markers: $T = 303$ K (open circle), $T = 323$ K (open square), and $T = 343$ K (open triangle). (b) Variation of the parameter A with the macroscopic stress Σ for three temperatures: $T = 303$ K (open circle), $T = 323$ K (open square), and $T = 343$ K (open triangle). The arrows in (a) point out the position of the maximum of A observed in (b).

dependence of the reinforcement will be called $R_{T_0,T}$. The temperature is rescaled in stress unit using the relation $K_y(T - T_0)$, where K_y was taken equal to 1 MPa K^{-1} and T_0 is the initial temperature. The stress dependence of the dynamical modulus measured at T_0, $R_{T_0,\Sigma}$ is directly plotted in Figures 6a and 7a. Each pair of curves ($R_{T_0,T}$, $R_{T_0,\Sigma}$) corresponds to a given initial temperature and thus merges at zero stress. To compare stress and temperature effects on reinforcement, it is convenient to define the function $A(\Sigma)$ which is the multiplicative factor applied to the stress such that $R_{T_0,\Sigma}(A(\Sigma)\Sigma)$ superimposes to $R_{T_0,T}(K_y(T - T_0))$.

Figures 6b and 7b show the variation of A with Σ determined from the comparison of the curves presented on Figures 6a and 7a. We observed that A goes through a maximum as the macroscopic stress amplitude increases. We will refer to them as A^{max} and Σ^{max}—the amplitude of A at its maximum and the corresponding value of Σ. To clearly visualize the position of this maximum on the R_Σ curves, we have pointed out the position of the maximum on the Figures 6a and 7a for all the temperatures T_0. This maximum corresponds to a decrease of the reinforcement of respectively about 80% and of 50% for the MCS_II and the ACS samples. The values of A are sensitive to temperature. For both the systems, Σ^{max} decreases and A^{max} increases with temperature. But the temperature dependence of the parameter A is strongly influenced by the particle dispersion state with a stronger sensitivity for the worse dispersion states. Actually, the absolute value of A and its variation with Σ are also extremely sensitive to the dispersion state. The values of A measured on the ACS samples (see Figure 7b)—very bad dispersion state—are 10 times larger than the ones obtained from the MCS_II samples (see Figure 6b)—bad dispersion state.

Let us note that, in the case of isolated particles where the local stress is nearly equal to the macroscopic one, the quantity A is expected to be constant and nearly equal to 1 but is actually very difficult to estimate by experiment.

C-2. Physical Meaning of Parameter A. Let us now comment the Figures 6b and 7b. The parameter A

exhibits a pronounced maximum as a function of the stress amplitude. We will try now to understand this effect in the frame of our glassy shell strain-softening approach. At first view, the parameter A can be considered as the amplification factor between the local stress and the average stress, in the glassy domains that are strain-softened. In fact, A is the average stress amplification, the average being performed on the local stress supported by the glassy domains that are strain-softened at a given amplitude. This strain-softened domains are obviously the one that supports most of the stress before the strain-softening, and the quantity A reflects the average amplification factor on the domains supporting the highest stress.

A is not easy to estimate, as it combines very local stress amplification, in bridges, and amplification over the size of aggregates composed of particles connected by glassy bridges. Let us here focused on this second effect.

To discuss more precisely this feature, let us first introduce here a hand waving argument that allows to compare temperature vs stress amplitude decrease of the elastic modulus. Let us consider a reinforced elastomer sample containing spherical particle as follows. We take all the pairs of neighboring particles. We will call "bonds" the set composed of two neighboring particles and the polymer matrix connecting them. All the bonds constitute a network, and each bond of the network has a specific elasticity and yield stress that depend on the distance between the particles surfaces, on temperature, and on the local stress. We can make the approximation that there is in fact two types of bonds, either glassy or rubberlike. The number of glassy, and thus rigid, bonds will depend on temperature and stress amplitude. We will also assume that the mechanical behavior of the sample is roughly the one of the network. Now when we increase the temperature from the glass transition temperature of the bulk T_g, we progressively decrease the number of rigid bonds by melting progressively the glassy polymer between the pair of particles. This decrease depends just on the distance distribution between pairs of particles. If, on the contrary, we increase the stress amplitude, we will strain-soften progressively the glassy bonds, depending not only on their length (distances between the two particles surfaces) but also on their local stress. Thus, the ratio between the strain-softening and the temperature decrease of glassy bonds, the factor A in our case, is nearly the amplification factor of the local stress carried by the bonds that are strain-softened. In the following we will assume that the factor A is about the stress-amplification factor that we have in our sample.

Now let us discuss the evolution of the amplification factor A vs temperature and stress amplitude.

Let us recall that in our bond-network picture, increasing the temperature for a given sample, starting from T_g, one progressively melts the glassy bonds. Thus, the network of glassy bonds will reach a percolation threshold at some temperature T_C. As a consequence, the amplification factor will be weak just above T_g and for very high temperature as drawn in Figure 8, and it will exhibit a maximum at T_C. The amplitude at the maximum and T_C will depend on the arrangement of the particles. If the arrangement is quite regular, crystalline for instance, the amplification factor will remain around 1. But if the system is more disordered, the amplification factor will exhibit a sharper maximum.

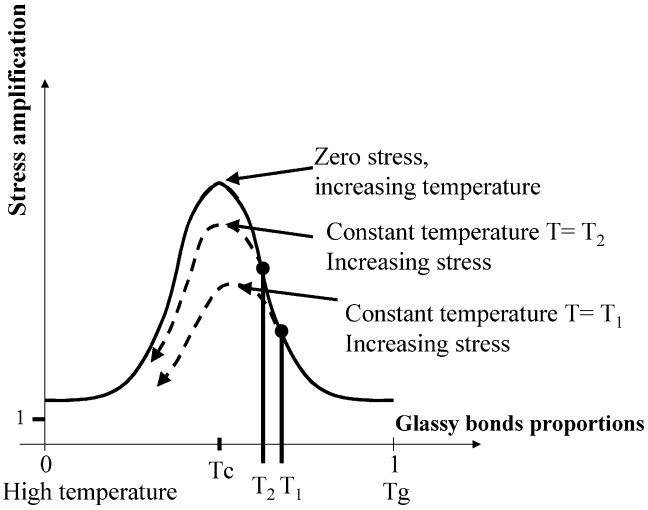

Figure 8. Schematic representation of the stress amplification factor vs the fraction of glassy bonds. While increasing temperature the glassy bonds are molten progressively, moving from right to left (solid line). The bond network goes through a percolation threshold at T_c. At this temperature, the stress localization and so the stress amplification are maximal. An increase of strain amplitude leads to a similar decrease of glassy bonds numbers. A bell-like shape for the amplification factor is obtained again (dashed line). However, in this case the amplification factor increases slower than for a temperature increase. The maximum of the amplification factor observed for increasing strain is then temperature dependent. It decreases as temperature increases (see the two dashed lines starting from temperatures T_1 and T_2 and Figure 6b).

The effect of the stress now can be compared in detail. A small temperature increase will soften bonds corresponding to a given distance between the particles surfaces and thus a given yield stress. This distance corresponds to the longest bridges that have not yet been melt. On the contrary, a small stress increase will strain-soften the bonds where the local stress is equal to the yield stress. In this last case, the most constrained glassy bridges will be preferentially softened.

As a consequence, an increase of temperature or stress is not equivalent for stress distribution in the system. From a rigid/soft bonds ratio r_1 at rest, we can reach a ratio r_2 lower than r_1 either by a temperature increase or by a stress increase (from right to left in Figure 8). However, the amplification factor at r_2 will depend on the followed path. It will be smaller in the case of stress increase than in the case of a temperature increase because any stress increase redistributes the stress more homogeneously than it was previously. This is schematically described in Figure 8. The solid line represents the amplification factor at zero stress for various increasing the ratio of glassy bonds or decreasing the temperature toward T_g. Obviously, this is valid for a given sample, but the shape of the curve will vary from sample to sample depending on anchorage between filler and matrix, volume fraction and arrangement of the fillers, nature of the polymer matrix, etc. However, a bell-like shape of the curve is always expected, whatever the sample. Let us plot the amplification factors at constant temperature, increasing the stress amplitude for respectively temperature T_1 and T_2 (in dashed line). The dashed line has to be below the solid one, as (see above) a stress amplitude increase decreases the stress localization. Hence, the maximum of the

amplification factor at $T_1 > T_2$ is larger from T_1 than for T_2. Moreover, the stress at which the amplification factor is maximum is smaller for T_1 than for T_2 because there are fewer bonds to strain-soften to reach the maximum of A.

Let us summarize the results of this naive approach: (i) We expect a bell-like shape for A that originates in a maximum of stress localization, corresponding to the percolation threshold for the glassy bonds network. (ii) We expect that the amplitude A^{max} will depend on the disorder of the particles arrangement. Characterizing the amplification factor, it must increase with the reinforcement in the linear regime, at a constant filler density and a similar polymer matrix. (iii) We expect that the amplitude A^{max} increases with temperature and simultaneously that the stress Σ^{max} decreases with temperature.

Actually, the three behaviors are observed in our samples. First, all the variations of A with the stress amplitude (see Figures 6a and 7a) exhibit a maximum. Second, the value at the maximum of A, A^{max}, is larger for ACS than for MCS_II (compare Figures 6b and 7b). Last, A^{max} increases with temperature while Σ^{max} decreases (see in Figure 7b). Thus, the factor A, even if it is probably not exactly the local stress amplification factor, describes an amplification of the local stress. Finally, a network picture is able to connect the bell-like shape of the A/Σ curves, the network being constituted by glassy bridges and elastic bridges between neighboring particles. Moreover, confirming the model, the temperature variation of A^{max} and of Σ^{max} qualitatively agrees with our experimental results, confirming once again the picture of a glassy polymer shell around each particle.

Conclusion

We have analyzed in this work the origin of the precocious nonlinear viscoelastic behavior observed on model filled elastomers composed by cross-linked poly(ethyl acrylate) chains reinforced with grafted silica nanoparticles. Our approach is based on the existence of a glass transition gradient near the particle surfaces. This approach, as shown in ref 13, accounts for the temperature and frequency variations of the linear viscoelastic modulus of filled elastomers. We show in this work that the precocious nonlinear viscoelastic behavior observed for increasing macroscopic deformation on these filled elastomers can be attributed to the strain-softening of a part of the glassy polymer that we have assumed to be similar to strain-softening in bulk at the corresponding T_g. In this frame, we can predict a temperature−frequency superposition law for the nonlinear elastic modulus that is validated by experiments. Moreover, we can compare the effect of temperature with the effect of strain amplitude on the softening of the glassy shells. It appears that the stress effect is quite complex. First, there is an important amplification factor between the macroscopic stress and the local stress. This is consistent with the fact that more disordered the sample is, the larger is the shift between stress and temperature dynamical modulus. Second, the shift factor between stress and temperature dynamical modulus exhibits a pronounced maximum which may correspond to the percolation threshold of the skeleton constituted by glassy bridges connecting neighboring particles. This is consistent with the variation of the mechanical behavior with temperature observed for our samples. When there is no stress amplification, i.e., in very well dispersed samples, the strain-softening should occur at very high macroscopic strain (≫100%) and should be weak. Last, all this picture explains the slow recovery of our samples after either a temperature quench (above T_g) or the cessation of a mechanical loading. It is also in agreement with the fact that the response becomes "apparently linear" after a few cycles. These last effects are in fact reminiscent from the properties of glassy polymers.

Finally, the effect of particles arrangements—on the precocious strain-softening, or Payne effect, in reinforced elastomers—remains still puzzling. We were able to show that the strain-softening of the glassy shells surrounding the solid particles is responsible for this effect in our filled elastomers. But we have also observed that its amplitude is very dependent on the arrangement of the particles through both the local stress amplification and the dependence of the local stress redistribution on the stress amplitude. Thus, we expect that new approaches taking precisely into account the particles arrangement under stress (like in 3), but including our effect of strain-softening of glassy chains, would be very efficient to describe the complex properties of filled elastomers.

Acknowledgment. We thank C. Fretigny for very helpful discussions.

References and Notes

(1) Kraus, G. *J. Appl. Polym. Sci., Appl. Polym. Symp.* **1984**, *39*, 75.
(2) Witten, T. A.; Rubinstein, M.; Colby, R. H. *J. Phys. II* **1993**, *3*, 367.
(3) Huber, G.; Vilgis, T. A. *Macromolecules* **2002**, *35*, 9204.
(4) Heinrich, G.; Klüppel, M.; Vilgis, T. A. *Curr. Opin. Solid State Mater. Sci.* **2002**, *6* 195.
(5) Maier, P. G.; Görizt, D. *Kautschuk Gummi Kunstoffe* **1996**, *49*, 18.
(6) Sternstein, S. S.; Zhu, A. J. *Macromolecules* **2002**, *35*, 7262.
(7) Struik, L. C. E. *Physical Aging in Amorphous Polymers and other Materials*; Elsevier: Amsterdam, 1978.
(8) Struik, L. C. E. *Polymer* **1987**, *28*, 1521.
(9) Haidar, B.; Vidal, A.; Papirer, E. *Proceeding, Eurofillers 97*, Manchester (UK) Sept 8−11, **1997**, 239. Haidar, B.; Salah Deradji, H.; Vidal, A.; Papirer, E. *Macromol. Symp.* **1996**, *108*, 147.
(10) Kaufmann, S.; Slichter, W. P.; Davis, D. D. *J. Polym. Sci., Part A2* **1971**, *9*, 829.
(11) Wang, M. J. *Rubber Chem. Technol.* **1998**, *71*, 520.
(12) Berriot, J.; Lequeux, F.; Monnerie, L.; Montes, H.; Long, D.; Sotta, P. *J. Non-Cryst. Solids* **2002**, *310*, 719.
(13) Berriot, J.; Montes, H.; Lequeux, F.; Long, D.; Sotta, P. *Macromolecules* **2002**, *35*, 9756.
(14) Keddie, J. L.; Jones, R. A. L.; Cory, R. A. *Europhys. Lett.* **1994**, *27*, 59.
(15) Forrest, J. L.; Dalnoki-Veress, K.; Dutcher, J. R. *Phys. Rev. E* **1997**, *56*, 5705.
(16) Fukao, K.; Miyamoto, Y. *Phys. Rev. E* **2000**, *61*, 1743.
(17) Grohens, Y.; Brogly, M.; Labbe, C.; David, M. O.; Schulzt, J. *Langmuir* **1998**, *14*, 2929.
(18) Starr, F. W.; Schröder, T. B.; Glotzer, S. C. *Macromolecules* **2002**, *35*, 4481.
(19) Starr, F. W.; Schröder, T. B.; Glotzer, S. C. *Phys. Rev. E* **2002**, *64*, 021802.
(20) Long, D.; Lequeux, F. *EPJ E* **2001**, *4*, 371.
(21) Payne, A. R. *Reinforcement of Elastomers*; Krauss, G., Ed., Wiley Interscience: New York, 1965; Chapter 3.
(22) Berriot, J.; Montes, H.; Mauger, M.; Martin, F.; Pyckhout-Hintzen, W.; Meier, G.; Frielinghaus, H. *Polymer*, in press.
(23) Jethmalani, J. M.; Ford, W. T. *Chem. Mater.* **1996**, *8*, 2138.
(24) Mauger, M. Thesis University Paris VI, 2000.
(25) Berriot, J.; Martin, F.; Montes, H.; Monnerie, L.; Sotta, P. *Polymer* **2003**, *44*, 1437.
(26) Berriot, J.; Montes, H.; Lequeux, F.; Pernot, H. *Polymer* **2002**, *43*, 6131.

(27) Ward, I. M. *Mechanical Properties of Solid Polymers*, 2nd ed.; John Wiley & Sons: New York, 1983.
(28) Ouali, N.; Mangion, M.; Perez, J. *Philos. Mag.* **1993**, *A67*, 827.
(29) Brule, B.; Halary, J. L.; Monnerie, L. *Polymer* **2001**, *42*, 9073.
(30) Zhou, Z.; Chudnovsky, A.; Bosnyak, C. P.; Sehanobish, K. *Polym. Eng. Sci.* **1995**, *35*, 304.
(31) Oleinik, E. F.; Shenogin, S. V.; Paramzina, T. V.; Rudnev, S. N.; Shantarovich, V. P.; Azamatova, Z. K.; Pakula, T.; Fischer, E. W. *J. Polym. Sci., Part A* **1998**, *40*, 1187.
(32) Rabinowitz, S.; Beardmore, P. *J. Mater. Sci.* **1974**, *9*, 81.
(33) Isayev, A. I.; Katz, D. *Int. J. Polym. Mater.* **1980**, *8*, 25.
(34) Chazeau, L.; Brown, J. D.; Yanyo, L. C.; Sternstein, S. S *Polym. Compos.* **2000**, *21*, 202.
(35) Lapra, A. Thesis University of Paris VI, 1999.
(36) For the strain field around a solid inclusion, see for instance: Palierne, J. F. *Rheol. Acta* **1990**, *29*, 204.
(37) Quinson, R.; Perez, J.; Rink, M.; Pavan, A. *J. Mater. Sci.* **1996**, *31*, 4387.
(38) Ricco, T.; Pegoretti, A. *J. Polym. Sci., Part B* **2002**, *40*, 236.

MA0344590